Alaskan soil carbon stocks: Spatial variability and dependence on environmental factors

Umakant Mishra[1*], William J. Riley[1]

[1]Earth Sciences Division, Lawrence Berkeley National Laboratory, 1 Cyclotron Road, 50A4037 Berkeley, CA 94720, USA.

Keywords: soil organic carbon, spatial variability, environmental control, active-layer, permafrost

Type of paper: Research article

[*]Corresponding author, tel: 510-495-2735, email:umishra@lbl.gov

Abstract

The direction and magnitude of soil organic carbon (SOC) changes in response to climate change depend on the spatial and vertical distributions of SOC. We estimated spatially-resolved SOC stocks to bedrock, distinguishing active-layer and permafrost-layer stocks, based on geospatial analysis of 472 soil profiles and spatially referenced environmental variables for Alaska. Total Alaska state-wide SOC stock was estimated to be 77 Pg, with 61% in the active-layer, 27% in permafrost, and 12% in non-permafrost soils. Prediction accuracy was highest for the active-layer as demonstrated by highest ratio of performance to deviation (1.5). Large spatial variability was predicted, with whole-profile, active-layer, and permafrost-layer stocks ranging from 1-296 kg C m^{-2}, 2-166 kg m^{-2}, and 0-232 kg m^{-2} respectively. Temperature and soil wetness were found to be primary controllers of whole-profile, active-layer, and permafrost-layer SOC stocks. Secondary controllers, in order of importance, were found to be: land cover type, topographic attributes, and bedrock geology. The observed importance of soil wetness rather than precipitation on SOC stocks implies that the poor representation of high-latitude soil wetness in Earth System Models may lead to large uncertainty in predicted SOC stocks under future climate change scenarios. Under strict caveats described in the text and assuming temperature changes from the A1B Intergovernmental Panel on Climate Change emissions scenario, our geospatial model indicates that the equilibrium average 2100 Alaska active-layer depth could deepen by 11 cm, resulting in a thawing of 13 Pg C currently in permafrost. The equilibrium SOC loss associated with this warming would be highest under continuous permafrost (31%), followed by discontinuous (28%), isolated (24.3%), and sporadic (23.6%) permafrost areas. Our high resolution mapping of soil carbon stock reveals the potential vulnerability of high-latitude soil carbon and can be used as a basis for future studies of anthropogenic and climatic perturbations.

Introduction

Soil organic carbon (SOC) can be a source or sink of atmospheric CO_2, with the current balance depending on climate, disturbance, soil characteristics, and vegetation. Reliable estimates of regional SOC stocks and their spatial and temporal variability are essential to better understand controls of SOC stocks and their vulnerability to changing climate. Of particular concern are high-latitude SOC stocks, which are preserved, in large part, because of low temperatures. High-latitude regions are expected to experience much higher temperature increases than temperate or tropical regions over the next century (IPCC, 2007) and therefore are a potentially vulnerable component of the global carbon cycle (Schuur *et al.,* 2008; McGuire *et al.,* 2009). Although uncertain, the total amount of frozen carbon in permafrost soils is estimated to be double (Schuur *et al.,* 2009; Tarnocai *et al.,* 2009) that currently in the atmosphere.

Several global SOC stock estimates exist for a variety of depth intervals (Post *et al.,* 1982; Batjes, 1996; Jobbagy & Jackson, 2000). However, these global estimates substantially underestimate permafrost affected SOC (Ping *et al.,* 2008a; Tarnocai *et al.,* 2009), mainly because of the paucity of high-latitude observations. Further, most of these studies limited the soil profile observations to the upper 1 m of soil profile even though high-latitude soils are reported to contain considerable deep SOC due to cryoturbation (Bockheim, 2007). Recent studies have also suggested the need for more accurate assessment of spatial heterogeneity of SOC stocks of permafrost-affected soils (Tarnocai *et al.,* 2009; Johnson *et al.,* 2011). To our knowledge, no regional high-latitude estimates exist of fine-resolution spatial variability of SOC stocks in the whole-profile (O to C horizons), active-layer, and permafrost-layer.

Previous estimates of SOC stocks in permafrost-affected soils have been made by stratifying the study area (e.g., by land cover type), averaging point observations of SOC stocks within each stratum, and multiplying by the aerial extent of that stratum (Ping *et al.*, 2008a; Tarnocai *et al.*, 2009; Johnson *et al.*, 2011). Outside of permafrost areas, this approach has been reported to be associated with high estimation errors because it does not represent soil and environmental variable heterogeneity within each strata (Thompson & Kolka, 2005; Meersmans *et al.*, 2008; Sanchez *et al.*, 2009). To address these concerns, McBratney *et al.* (2003) proposed a framework to predict the spatial distribution of SOC using spatially referenced "scorpan" factors (soil properties, climate, organisms, relief, parent material, age, and spatial coordinate). Several subsequent studies have demonstrated that this approach results in more accurate representation of spatial variability of soil properties and reduction of prediction errors (Thompson & Kolka, 2005; Rasmussen, 2006; Meersmans *et al.*, 2008).

Spatially-distributed observations of permafrost SOC stocks are important for development and testing of Earth System Model (ESMs). Several recent modeling studies have integrated improved representation of high-latitude SOC dynamics (e.g., Lawrence *et al.*, 2008; Schaeffer *et al.*, 2011; Koven *et al.*, 2011), but substantial differences remain between these ESM estimates and the coarse-resolution observationally-based SOC estimates mentioned above. These differences occur because of uncertainties associated with spatially extrapolating limited observations and several limitations with the ESM modeling approaches, including lack of vertical resolution of SOC stocks, differing environmental controls of existing SOC stocks, unrealistic spatial representation to infer soil variability, and lack of pedogenic processes typical of high-latitude environments such as cryogenic aggregation, podzolization, and cryoturbation. Despite these limitations, ESMs are often used to predict carbon-climate feedbacks, although

they predict very large ranges in permafrost SOC losses under future warming scenarios (25 - 85 Pg C) depending upon the processes included in the models (Koven *et al.*, 2011).

Here, we used spatially referenced environmental variables (topographic attributes, land cover types, climate, and bedrock geology), and observed SOC pedon description data in a geographically weighted regression (GWR) approach to predict the spatial variability of SOC stocks and prediction accuracy throughout Alaska. Our approach allowed us to separately estimate active and permafrost-layer SOC stocks at 60 m spatial resolution, and to analyze the spatial variability under continuous, discontinuous, sporadic, and isolated permafrost regions. We also present predicted environmental controls on SOC stocks, and used them to estimate expected changes in equilibrium 2100 SOC stocks associated with the moderate A1B Intergovernmental Panel on Climate Change (IPCC) emissions scenario (IPCC, 2007).

Materials and methods

SOC profile observations

We used 422 geo-referenced SOC profile data from the National Soil Survey Characterization database (NSSL, 2010). This soil survey database includes measured representative soil profiles from Alaska and covered all soil types at the soil suborder level (18 suborders). We included an additional 50 soil profile observations from the Arctic regions of North America (Ping *et al.*, 2008a). Though the SOC profile samples were unevenly distributed throughout the study area (Fig. S1), the samples covered all 27 major land resource areas (MLRA) of Alaska. The MLRA is a geographical unit that contains similar patterns of climate, soils, water resources, and land uses (SCS, 1981). Since our objective was to estimate the SOC stock across Alaska, we included

all the pedon description data in our study. Unfortunately, the majority of the pedon description data did not include bulk density observations. Therefore the bulk density of each soil horizon was estimated using soil texture, depth, and organic matter content using pedotransfer functions developed by Calhoun *et al.* (2001) and Adams (1973). The SOC stock for each profile was estimated by summing the SOC stock from the surface to the C horizon:

$$C_T = \sum_{j=1}^{n} C_j \ \rho_b \ \mathrm{D}_j$$

where C_T = SOC stock (kg m^{-2}) of the whole soil profile, j = soil horizon number (1, 2, 3, ..., n), C_j is the SOC concentration (kg kg^{-1}), ρ_b is the soil bulk density corrected for rock fragments (kg m^{-3}), and D_j is the thickness of each horizon (m).

In the soil dataset, the presence of a permafrost layer was indicated by horizon "f" (i.e., frozen layer). We used the average depth of the "f" horizon to determine the boundary between permanently frozen and active layers (Table S1).

Environmental datasets

A digital elevation model (DEM) of 60 m spatial resolution was obtained from the USGS database (Multi-Resolution Land Characteristics Consortium, 2010). From the DEM we calculated 13 terrain attributes that are useful to predict the SOC stock across environmental conditions (using the spatial Analyst function of ArcGIS version 10, Environmental Systems Research Institute, Inc., Redlands, CA, USA). These indices include elevation, slope, aspect, curvature (plan, profile, and total), upslope contributing area, flow length, soil wetness index, sediment transport index, stream power index, terrain characterization index, and slope aspect

index. From the 13 topographic attributes, 4 attributes were selected for the model calibration in the best subset regression approach (Kutner *et al.*, 2004). The included topographic attributes were elevation (meters), specific catchment area (A_s, $m^2\ m^{-1}$), soil wetness index (SWI), and sediment transport index (STI). Specific catchment area is the upslope area per unit width of contour (Wilson & Gallant, 2000). The SWI indicates the spatial distribution and extent of zones of soil water saturation and is calculated as the ratio of specific catchment area to slope gradient (β, degrees) (Wilson & Gallant, 2000):

$$SWI = \left(\frac{A_s}{\tan \beta} \right)$$

The sediment transport index (STI) resembles the slope-length factor of the Universal Soil Loss Equation and characterizes erosional and depositional areas and potential erosion risk (Wilson & Gallant, 2000) :

$$STI = \left(\frac{A_s}{22.13} \right)^{0.6} \left(\frac{\sin \beta}{0.0896} \right)^{1.3}$$

Land cover data of 60-m spatial resolution was extracted for Alaska from the NLCD database (Multi-Resolution Land Characteristics Consortium, 2010). We reclassified the NLCD land cover types into 9 major categories (Table S2). The largest land area was under the scrub category (43%), followed by forest (25%), barren (8.5%), herbaceous (7%), and wetlands (7%). The remaining surface area (9.5%) was under open water, perennial ice, barren land, and moss vegetation. Indicator variables for the presence or absence of 7 land cover types (except open water and perennial ice) were created and used in the model selection process.

The climate data, such as the long-term (1961-1990) mean annual air temperature and mean annual precipitation, were obtained from the PRISM database of spatial climate analysis service of the Oregon State University (Daly *et al.,* 2001). The bedrock geology data was obtained from a USGS database (Beikman, 1980). Across Alaska there were 180 types of bedrock. The largest land area was under quaternary deposits (8%), followed by Cretaceous rocks (7.3%), Lower paleozoic rocks (6.6%), Lower cretaceous rocks (6.2%), ice (4.3%), and Pleistocene deposits (4.2%). The remaining surface area was under the remaining 174 bedrock types.

Spatial modeling and accuracy of prediction

We used a GWR approach (Fotheringham *et al.,* 2002; Mishra *et al.,* 2010; Zhang *et al.,* 2011) and geospatial analysis to predict Alaska SOC stocks. First, the best subset regression was used to identify the environmental variables using a Mallow's C_p criteria (Kutner *et al.,* 2004). The model was tested for multicollinearity of selected independent variables, unequal error variance, normality, and randomness of the residuals. In this analysis, all the data points contributed to the estimates of model parameters equally using a least square solution. SAS statistical software (SAS, 2004) was used for model selection. The selected independent variables were then used in a GWR approach to derive the spatially varying model parameters at a 1000 m regular interval throughout the study area. In GWR, the weight function was chosen as an adaptive spatial kernel type so that the spatial extent for included samples varied based on sample density. The bandwidth was chosen based on Akaike Information Criterion minimization (Fotheringham *et al.,* 2002). The GWR procedure can be represented as:

$$\hat{SOC}_i = \hat{\beta}_0(u_i, v_i) + \hat{\beta}_1(u_i, v_i)X_{i1} + \hat{\beta}_2(u_i, v_i)X_{i2} + \cdots\cdots + \hat{\beta}_k(u_i, v_i)X_{ik} \qquad (4)$$

where $\hat{SOC}_i$ is the predicted SOC stock at location i; (u_i, v_i) are the coordinates for location i; k is the number of environmental variables, $\hat{\beta}_0$ - $\hat{\beta}_k$ are regression coefficients; and X_{i1} to X_{ik} are environmental variables at location i (Table S3 and S4).

We evaluated the prediction accuracy of the resulting SOC stock maps by using a K-fold validation approach (Mishra *et al.*, 2010; Martin *et al.*, 2011). In this approach, the entire dataset was randomly divided into calibration (n=412) and validation (n=60) datasets five times. Mapping of SOC using calibration datasets and their validation were conducted for each split and the average validation indices are reported here. From the predicted SOC maps, SOC stock values were extracted for the validation points. The obtained values of observed and predicted C pool were interpreted by calculating different validation indices, such as the mean estimation error (*MEE*) and root mean square error (*RMSE*):

$$MEE = \frac{1}{n}\sum_{i=1}^{n}(\hat{C}_s(x_i) - C_s(x_i))$$

$$RMSE = \sqrt{\frac{1}{n}\sum_{i=1}^{n}(\hat{C}_s(x_i) - C_s(x_i))^2}$$

where $C_s(x_i)$ is the measured SOC stock, $\hat{C}_s(x_i)$ is the estimated SOC stock, and n is the number of validated observations. These values should approach zero for an optimal prediction. We also calculated the ratio of performance to deviation (RPD; defined as the ratio between the

standard deviation and the RMSE), which indicates the overall prediction ability of the selected approach.

Environmental controls on SOC stocks were examined by converting temperature, precipitation, and elevation data into zones and then calculating the SOC stocks of active-layer, permafrost-layer, and whole-profile layers in each zone. Similar calculations were performed for land cover type impacts on SOC stocks. The impact of future warming on SOC stocks was evaluated using anticipated temperature changes under the moderate emission scenario (A1B) of IPCC (citation). The downscaled future temperature change projections for Alaska were obtained from the Scenarios Network for Alaska Planning (SNAP, 2011). This dataset provides a five model composite values (IPCC predictions: selected on the basis of smallest systematic errors) at a 2 km grid across Alaska.

Results and discussion

Spatial and vertical distribution of soil organic carbon stocks

In this section we discuss the predicted distribution of SOC stocks; estimates of the controls on SOC stocks are discussed in the following section. Predicted whole-profile SOC stocks had high spatial variability (coefficient of variability, CV = 49%), ranging from 1 to 296 kg m^{-2} with an average across Alaska of 53.6 kg m^{-2} (Fig. 1a). The Northern and Western regions of Alaska had the highest predicted levels of whole-profile SOC (>75 kg m^{-2}) (Fig. 1a). The Eastern and Southern regions had the lowest whole-profile SOC stocks (< 50 kg m^{-2}). The average prediction error for whole-profile SOC stock was 26.3 kg m^{-2} and the observed ratio of

performance to deviation (RPD) was 1.4, indicating our approach has a moderate predictive ability for whole-profile SOC stocks (Gomez *et al.,* 2008). The predicted average Alaska active-layer SOC stock was 35.4 kg m^{-2}, ranging from 2 to 166 kg m^{-2} (Fig. 1b). Active-layer SOC stocks also had high spatial variability (CV=59%). The average error of prediction for active-layer SOC stock was 17.8 kg m^{-2} and the RPD was 1.5. Predicted permafrost SOC stock ranged from 0 to 232 kg m^{-2} with a spatial average of 21.3 kg m^{-2} and the highest spatial variability (CV=108%) (Fig. 1c). The observed average error of prediction was 36.6 kg m^{-2} and the RPD was 0.93 (Table 1). Our results suggest, on average across the state, a larger proportion of soil organic carbon is stored in the active-layer than in the permafrost layer. Whole-profile SOC stocks across Alaska, excluding underneath water and glaciers, were estimated to be 77 Pg, of which 47 Pg are in the active layer, 21 Pg are in the permafrost layer, and 9 Pg are in perennially unfrozen areas. Of the 21 Pg permafrost SOC stock, 14, 5, 1, and 1 Pg are under continuous, discontinuous, sporadic, and isolated permafrost areas, respectively (Table 2).

Our estimates of Alaska whole-profile SOC stocks are higher than previously published studies (Post *et al.,* 1982; Ping *et al.,* 2008a; Tarnocai *et al.,* 2009; Johnson *et al.,* 2011). Several factors contributed to the differences with these previous studies: we included more observations, our estimates were not limited to a relatively shallow depth interval, and we used a geospatial prediction approach that is more accurate than the spatial extrapolation methods of previous studies (McBratney *et al.,* 2003; Thompson & Kolka, 2005; Meersmans *et al.,* 2008; Sanchez *et al.,* 2009). For comparison, Post *et al.* (1982) used 48 samples and reported an average SOC value of 21.8 kg m^{-2} for the Arctic tundra region (our estimate was 3 times as large for the same region). The samples used in that study were primarily from shallow depth, only 30 samples were from a depth of 100 cm, and none of the samples were from below 100 cm. Ping *et*

al. (2008a) used 117 1-meter deep samples from northern Alaska (north of 60°N) and reported average SOC stocks to be 34.8 kg m^{-2}, 21.7 kg m^{-2}, and 13.1 kg m^{-2} for 1 m depth, active, and permafrost layers, respectively (compared to our estimates which were 1.8, 1.5, and 2.3 times as large, respectively, for the same region). Though Ping *et al.* (2008a) were the first to report SOC stocks in different depth intervals from arctic soils, they did not provide information about whole soil profile SOC stocks (down to bedrock). Tarnocai *et al.* (2009) used 131 observations from Alaskan soils and reported 18 Pg of SOC stock to 3 m depth. However, this study did not differentiate the SOC stocks into active and permafrost layers and assigned no SOC to the non-permafrost affected soils of Alaska (322,629 km^2) where we predicted a range of 0-20 kg m^{-2} SOC. Finally, Johnson *et al.* (2011) stratified the state of Alaska into ecoregions and reported average SOC stocks to 1 m depth of 53.3 kg m^{-2}, 8.6 kg m^{-2}, 21 kg m^{-2}, and 24 kg m^{-2} for arctic tundra, intermontane boreal, Alaska range transition, and coastal rainforests, respectively (our estimates were 1.3, 5.8, 1.5, and 1.6 times as large for the same ecoregions). Although these studies grouped regions differently and covered different areas of Alaska, our SOC stock estimates were between 1.3 and 5.8 times as large when comparable groupings were considered.

For comparison with whole-profile and permafrost-layer SOC stocks, we attribute differences between our results and these previous studies to the relatively deeper profiles we considered. Of the 472 SOC profiles we examined, 339 were non-permafrost affected profiles; of these, 180 (53%) were deeper than 1 m. Of the remaining 133 permafrost-affected profiles, 76 (57%) and 8 (6%) were deeper than 1 and 3 m (up to 4.5 m), respectively. Because including these deeper profiles in our estimate led to substantially higher predicted whole-profile and permafrost-layer SOC stocks, we believe that these previous studies underestimated these portions of Alaskan SOC stocks. For active-layer SOC stocks, we attribute our ~1.5 times larger

predictions to our geospatial non-stationary prediction approach, which considers the impact of the spatial heterogeneity of SOC controllers in contrast with these previous studies.

Controls on soil organic carbon stocks

We found that whole-profile, active-layer, and permafrost SOC stocks decreased with increased elevation (Fig. 2), and most SOC stocks (70%) were located in areas with elevation below 400 m. Low elevation areas throughout Alaska are associated with lower slope gradients and higher soil wetness, both of which were predictors of higher SOC stocks. This result is consistent with observations made by Ping *et al.* (2008a) who reported higher total SOC stocks in low elevation areas of Alaska north of 60 ^{o}N.

Annual-average temperature was strongly related to active-layer and permafrost-layer SOC stocks: As the 30-year annual-average air temperature increased from -18 to 0^{o}C, active-layer SOC stock increased and permafrost-layer SOC stock decreased. Between 0 and 4^{o}C, the increase in predicted permafrost-layer SOC stock was due to inclusion of sporadic (14% of Alaska surface area) and isolated (85% of Alaska surface area) permafrost areas located in this temperature range. Both the active-layer and permafrost-layer SOC stocks decreased in the 4 to 6^{o}C range. Whole-profile SOC stocks decreased with increased annual-average temperature (Fig. S2). Our predicted control of temperature on the spatial distribution of whole-profile SOC stocks across Alaska is similar to the findings of other studies that reported negative relationships of air temperature to SOC stocks (Ping *et al.,* 2008a; Johnson *et al.,* 2011). The common explanation for this negative dependence is cryoturbation, i.e., subduction of surface SOC into the soil matrix due to seasonal freeze and thaw, and protection of this SOC from mineralization and decomposition due to freezing temperatures (Michaelson *et al.,* 1996; Ping *et al.,* 2008b).

Predicted whole-profile SOC stock decreased with increased precipitation up to 800 mm per year and then remained constant (Fig. S3). However, no trend was observed for active-layer and permafrost SOC stocks with precipitation. Our findings are consistent with observations reported by Guo *et al.* (2006) in the conterminous US, who also reported no consistent relationships with increasing precipitation. Since the dominant proximal hydrological control on SOC decomposition in upland systems is soil moisture and not directly precipitation, we used topographic wetness index as a soil moisture proxy in our spatial extrapolation approach. Predicted whole-profile and active-layer SOC stocks were strongly related to this index (Fig. S4). We believe that the observed importance of soil wetness rather than precipitation on SOC stocks implies that the poor representation of high-latitude soil wetness in Earth System Models (Lawrence & Slater, 2005; Schaefer *et al.*, 2011) may lead to large uncertainty in predicted SOC stocks under future climate change scenarios.

Among different land cover types, herbaceous vegetation had the highest Alaska-average whole-profile, active-layer, and permafrost SOC stocks (Fig. 3). After herbaceous vegetation, scrub and wetlands had the highest whole-profile SOC stocks. Barren land had the lowest predicted whole-profile, permafrost-layer, and active-layer SOC stocks in Alaska. These low stocks are likely due to low vegetation cover (<15%), and therefore low productivity, and high-elevation and high-slope positions, and therefore high erosional losses.

Impact of possible temperature changes on equilibrium Alaska carbon stocks

Using the relationships we derived from the 472 pedons and controlling environmental variables described above, we estimated the equilibrium impact of anticipated temperature

changes on SOC stocks and active layer thickness for the IPCC A1B 2100 climate. We note several important assumptions to this equilibrium SOC stock estimate: (1) current SOC stocks are related to the 30-year average climate and current vegetation and soil distributions used to develop the spatial extrapolation of individual pedons to all of Alaska as described above; (2) the estimated changes in SOC stocks reflect a new equilibrium state consistent with the new atmospheric temperature (i.e., SOC stocks have enough time to re-equilibrate with the new imposed climate, a process that can take many centuries); and (3) that interaction terms (e.g., between temperature, precipitation, vegetation distribution, and gross and net primary production) are neglected. Since none of these assumptions are likely to be fully realized, we consider the resulting estimates to be relatively uncertain. We note, however, that other methods used to predict changes in high-latitude SOC stocks under a changing climate, such as land-surface models integrated in global circulation models (Lawrence & Slater, 2010; Schaefer *et al.*, 2011; Riley *et al.*, 2011; Koven *et al.*, 2011), come with their own equally restrictive, and occasionally acknowledged, assumptions. With these caveats in mind, and assuming an A1B IPCC temperature scenario at 2100, we estimated that the equilibrium Alaska-average active-layer thickness could deepen by 11 cm, thawing ~13 Pg of permafrost SOC with an associated 27% loss of permafrost area throughout Alaska. The corresponding whole-profile permafrost SOC loss was estimated to be 31, 28, 24, and 24% from continuous, discontinuous, isolated, and sporadic permafrost areas, respectively. The impact of warming was highest in the northeastern part of Alaska (dominated by continuous permafrost) and lowest in the southwestern part (dominated by sporadic permafrost). The 30-year annual-average temperature in these areas ranged from -10 to -4^{o}C and -4 to 0^{o}C, respectively.

Modeling studies of permafrost loss and active layer thickness increases either for Alaska or for the Northern Hemisphere under the same emissions scenario (A1B) varied widely. For Northern Hemisphere permafrost area, Saito *et al.* (2007), Lawrence & Slater (2010), Lawrence *et al.* (2008), and Schaefer *et al.* (2011) predicted 40-57%, 73-88%, 80-85%, and 20-39% reductions, respectively. For Alaska, Marchenko *et al.* (2008) and Schaefer *et al.* (2011) predicted 7% and 22-61% permafrost area reduction, respectively. The projected range of increases in active-layer depth from these studies is also broad, ranging from 50-300 cm. The large differences between these previous model projections are likely due to differences in model process representation, whether they included specific mechanisms (e.g., fire), climate forcing (e.g., snow and precipitation inputs, air temperatures), and the strength of land-atmosphere feedbacks. Direct comparisons with our results are complicated because these studies analyzed a larger region and attempted to include other factors that can impact permafrost SOC stocks, e.g., changes in hydrology, fire, growing season length, and others. Unfortunately, none of these numerical modeling studies reported results for simulations that can be directly compared to our estimates, which attempted to account for only the effects of changing temperature. Nevertheless, our predicted loss of permafrost area is at the lower end of the range of these studies, and our predicted increase in average active-layer thickness is lower than these previous estimates.

Limitations of predicted SOC stocks

Our prediction accuracy of current SOC stocks was constrained by the limited number of available SOC profile observations, their uneven distribution across Alaska, and variations in the time of observation (most of the samples were taken between 1975 and 1990). Likewise, we

were not able to apply all relevant soil forming factors (environmental variables) since spatially-resolved observations of, for example, fire frequency, fire intensity, and time of soil formation do not exist for much of Alaska. Future work should address the role these other factors have on high-latitude SOC stocks.

Conclusions

Our geospatial analysis using SOC profile observations and potential environmental and ecosystem controllers led to higher predicted Alaska SOC stocks than previously reported. We attribute the increase to our inclusion of deeper SOC profile observations, spatially heterogeneous environmental parameters, and non-stationary spatial modeling approach. Temperature and soil wetness were primary controllers on whole-profile, active-layer, and permafrost-layer SOC stocks. Secondary controllers, in order of importance, were: land cover type, topographic attributes, and bedrock geology. The large spatial heterogeneity of these factors across Alaska led to very large predicted spatial variability in SOC stocks. We also estimated, with important caveats, potential equilibrium SOC losses associated with a moderate temperature change scenario (A1B). Our estimates of potential permafrost area loss and active-layer thickening were at the lower end of, and below, respectively, previously reported values from earth system modeling analyses. Because of the caveats discussed above regarding the use of current observations to infer future conditions, analyses with mechanistic land-surface models are the only practical approach to accurately estimating future SOC stocks. However, since no current ESM accurately reproduces high-latitude SOC stocks, spatially-distributed datasets based on observations, such as that reported here, are an important step toward improving and testing these models.

Acknowledgements

This study was supported by the Director, Office of Science, Office of Biological and Environmental Research, Climate and Environmental Science Division, of the US Department of Energy under Contract No. DE-AC02-05CH11231 to Berkeley Lab. Thanks to G. Michaelson and M. T. Jorgenson for providing access to some of the SOC profile data and layer of permafrost cover respectively.

References

Adams WA (1973) The effect of organic matter on the bulk and true densities of some uncultivated podzolic soils. *Journal of Soil Science*,**24,**10-17.

Batjes NH (1996) Total carbon and nitrogen in the soils of the world. *European Journal of Soil Science*, **47,** 151-163.

Beikman HM (1980) Geologic Map of Alaska, U.S. Geological Survey. scale 1:2,500,000 (http://agdc.usgs.gov/data/usgs/geology/index.html).

Bockheim JG (2007) Importance of cryoturbation in redistributing organic carbon in permafrost-affected soils. *Soil Science Society of America Journal*, **71,** 1335-1342.

Calhoun FG, Smeck NE, Slater BK, Bigham JM, Hall GF (2001) Predicting bulk density of Ohio soils from morphology, genetic principles, and laboratory characterization data. *Soil Science Society of America Journal*,**65,** 811-819.

Daly C, Taylor GH, Gibson WP, Parzybok TW, Johnson GL, Pasteris P (2001) High quality spatial climate data sets for the United States and beyond. *Transactions of the American Society of Agricultural Engineers*,**43,** 1957-1962.

Fotheringham AS, Brunsdon C, Charlton M (2002) *Geographically weighted regression the analysis of spatially varying relationships.* John Wiley & Sons, UK .

Gomez C, Rossel RAV, McBratney AB (2008) Soil organic carbon prediction by hyperspectral remote sensing and field vis-NIR spectroscopy: An Australian case study. *Geoderma*, **146,** 403-411.

Guo Y, Gong P, Amundson R, Yu Q (2006) Analysis of factors controlling soil carbon in the conterminous United States. *Soil Science Society of America Journal*, **70,** 601-612.

IPCC 2007. Summary for policy makers. In: *Climate change 2007: The physical science basis.* Contribution of Working Group 1 to the Fourth Assessment Report of the Intergovernmental Panel on Climate Change. Cambridge University Press, New York.

Jobbagy EG, Jackson R B (2000) The vertical distribution of soil organic carbon and its relation to climate and vegetation. *Ecological Applications*, **10,** 423-436.

Johnson KD, Harden J, McGuire AD *et al.* (2011) Soil carbon distribution in Alaska in relation to soil-forming factors. *Geoderma*, **167,** 71-84.

Koven CD, Ringeval B, Friedlingstein P *et al.* (2011) Permafrost carbon-climate feedbacks accelerate global warming. *Proceedings of the National Academy of Sciences of the United States of America*, **108,** 14769-14774.

Kutner MH, Nachtsheim CJ, Neter J (2004) *Applied linear regression models*, McGraw-Hill, New York.

Lawrence DM, Slater AG (2005) A projection of severe near-surface permafrost degradation during the 21st century. *Geophysical Research Letters,* **32,** L24401.

Lawrence DM, Slater AG (2010) The contribution of snow condition trends to future ground climate. *Climate Dynamics,* **34,** 969-981.

Lawrence DM, Slater AG, Romanovsky VE, Nicolsky DJ (2008) Sensitivity of a model projection of near-surface permafrost degradation to soil column depth and representation of soil organic matter. *Journal of Geophysical Research,* **113,** F02011.

Marchenko S, Romanovsky V, Tipenko G (2008) Numerical modeling of spatial permafrost dynamics in Alaska. *Proceedings Ninth International Conference on Permafrost,* **2,** 1125-1130.

Martin MP, Wattenbach M, , Smith P, Meersmans J, Jolivet C, Boulonne L, Arrouays D, (2011) Spatial distribution of soil organic carbon stocks in France. *Biogeosciences,* **8,** 1053-1065.

McBratney AB, Mendonça-Santos ML, Minasny B (2003) On digital soil mapping. *Geoderma,* **117,** 3-52.

McGuire AD, Anderson LG, Christensen TR *et al.* (2009) Sensitivity of the carbon cycle in the Arctic to climate change. *Ecological Monographs,* **79,** 523-555.

Meersmans J, De Ridder F, Canters F, De Baets S, Van Molle M (2008) A multiple regression approach to assess the spatial distribution of soil organic carbon (SOC) at the regional scale (Flanders, Belgium). *Geoderma,* **143,**1-13.

Michaelson GJ, Ping CL, Kimble JM (1996) Carbon storage and distribution in tundra soils of arctic Alaska, U.S.A. *Arctic and Alpine Research,* **28,** 414-424.

Mishra U, Lal R, Liu D, Van Meirvenne M (2010) Predicting the spatial variation of soil organic carbon pool at a regional scale. *Soil Science Society of America Journal,***74,** 906-914 (2010).

Multi-Resolution Land Characteristics Consortium (2010) *National land cover database 2001*. Available at www.epa.gov/mrlc/nlcd-2001.html (Accessed on Apr 3 2010). USEPA, Washington, DC.

National Soil Survey Laboratory (2010) Soil characterization database. Available at http://ssldata.nrcs.usda.gov/ (Accessed on Mar 6, 2010).

Ping CL, Michaelson GJ, Jorgenson MT, Kimble JM, Epstein H, Romanovsky VE, Walker DA (2008a) High stocks of soil organic carbon in the North American arctic region. *Nature Geoscience,* **1,** 615-619.

Ping CL, Michaelson GJ, Kimble JM, Romanovsky VE, Shur YL, Swanson DK, Walker DA (2008b) Cryogenesis and soil formation along a bioclimate gradient in Arctic North America. *Journal of Geophysical Research,* **113,** G03S12.

Post WM, Emanuel WR, Zinke PJ, Stangenberger AG (1982) Soil carbon pools and world life zones. *Nature,* **298,** 156 -159.

Rasmussen C (2006) Distribution of soil organic and inorganic carbon pools by biome and soil taxa in Arizona. *Soil Science Society of America Journal,***70,** 256-265.

Riley WJ, Subin ZM, Torn MS *et al.* (2011) Barriers to predicting changes in global terrestrial methane fluxes: Analyses using CLM4ME, a methane biogeochemistry model integrated in CESM. *Biogeosciences, **8,*** 1925-1953.

Saito K, Kimoto M, Zhang T, Takata K, Emori S (2007) Evaluating a high-resolution climate model: simulated hydrothermal regimes in frozen ground regions and their change under the global warming scenario. *Journal of Geophysical Research,***112,** doi:10.1029/2006jf000577.

SAS Institute Inc. *Statistical analysis software version 9.1.3 for micro computers* (SAS Institute Inc., NC, 2004).

Sanchez PA, Ahamed S, Carre F *et al.* (2009) Digital soil map of the world. *Science,* **325,** 680-681.

Scenarios Network for Alaska planning (2011) Available at http://www.snap.uaf.edu (Accessed on Apr 6, 2010).

Schaefer K, Zhang T, Bruhwiler L, Barrett AP (2011) Amount and timing of permafrost carbon release in response to climate warming. *Tellus,* **63B,** 165-180.

Schuur EAG, Bockheim J, Canadell JG *et al.* (2008) Vulnerability of permafrost carbon to climate change: Implications for the global carbon cycle. *BioScience,* **58,** 701-714.

Schuur EAG, Vogel JG, Crummer KG, Lee H, Sickman JO, Osterkamp TE (2009) The effect of permafrost thaw on old carbon release and net carbon exchange from tundra. *Nature,* **459,** 556-559.

Soil Conservation Service. 1981. *Land resource regions and major land resource areas of the United States*. Agriculture Handbook 296, U.S. Gov. Print. Office, Washington, DC.

Tarnocai C, Canadell JG, Schuur EAG, Kuhry P, Mazhitova G, Zimov S (2009) Soil organic carbon pools in the north circumpolar permafrost region. *Global Biogeochemical Cycles,* **23,** GB203.

Thompson JA, Kolka RK (2005) Soil carbon storage estimation in a forested watershed using quantitative soil landscape modeling. *Soil Science Society of America Journal,***69,**1086-1093.

Wilson JP, Gallant JC (2000) Digital terrain analysis. In: *Terrain Analysis* (eds Wilson JP, Gallant JC), pp. 1-27. John Wiley and Sons, New York.

Zhang C, Tang Y, Xu X, Kiely G (2011) Towards spatial geochemical modeling: Use of geographically weighted regression for mapping soil organic carbon contents in Ireland. *Applied Geochemistry* doi:10.1016/j.apgeochem.2011.04.014.

Supporting Information Legends

Figure S1. Distribution of soil organic carbon profile observations across Alaska.
Figure S2. Average SOC stocks in each temperature zone. Error bar is the standard deviation.

Figure S3. Average SOC stocks in each precipitation zone. Error bar is the standard deviation.

Figure S4. Average SOC stocks in each soil wetness zone. Error bar is the standard deviation.

Table S1. Descriptive statistics of observed soil organic carbon (SOC) stocks (total dataset, n=472; permafrost profiles, n=133)

Table S2. Reclassification of USGS land-cover types for this study.

Table S3. Geographically weighted regression model summary for log transformed whole profile SOC stocks.

Table S4. Geographically weighted regression model summary for log transformed active layer SOC stocks.

Table 1. Prediction accuracy of soil organic carbon stocks of different depth intervals.

Soil organic carbon		*Validation errors*	
Stocks (kg m^{-2})	*MEE*	*RMSE*	*RPD*
Whole Profile	-5.7	26.3	1.4
Active layer	3.2	17.8	1.5
Permafrost	11.2	37.6	0.9

MEE is Mean estimation error; RMSE is root mean square error; RPD is ratio of performance to deviation.

Table 2. Soil organic carbon stocks in different depth intervals and permafrost zones across Alaska (NA = not applicable).

Permafrost Category	*Whole Profile (Pg)*	*Active Layer (Pg)*	*Permafrost Layer (Pg)*
Continuous	32	18	14
Discontinuous	22	17	5
Sporadic	7	6	1
Isolated	7	6	1
Unfrozen areas	9	NA	NA

Figure Legends

Figure 1. Predicted soil organic carbon stocks in (a) whole-profile, (b) active-layer, and (c) permafrost layers in Alaska.

Figure 2. Average whole-profile, active-layer, and permafrost SOC stocks in each elevation zone of Alaska. Error bar is the standard deviation and n is the number of observations.

Figure 3. Predicted average whole-profile, active-layer, and permafrost SOC stocks under different land covers in Alaska. Error bar is the standard deviation and n is the number of observations .

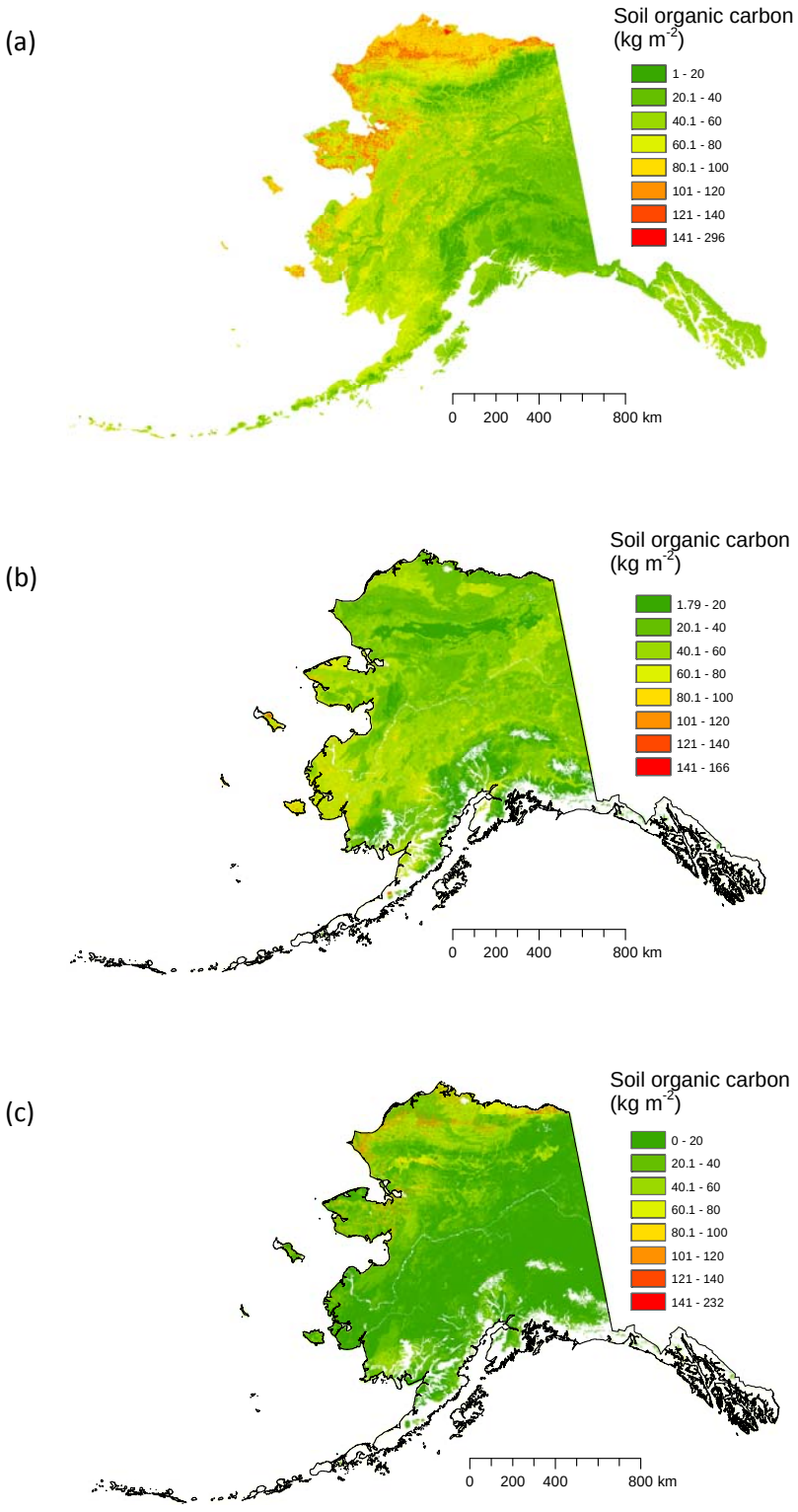
(a)
Soil organic carbon
(kg m-2)
1 - 20
20.1 - 40
40.1 - 60
60.1 - 80
80.1 - 100
101 - 120
121 - 140
141 - 296
0 200 400 800 km
(b)
Soil organic carbon
(kg m-2)
1.79 - 20
20.1 - 40
40.1 - 60
60.1 - 80
80.1 - 100
101 - 120
121 - 140
141 - 166
0 200 400 800 km
(c)
Soil organic carbon
(kg m-2)
0 - 20
20.1 - 40
40.1 - 60
60.1 - 80
80.1 - 100
101 - 120
121 - 140
141 - 232
0 200 400 800 km

Figure 1.

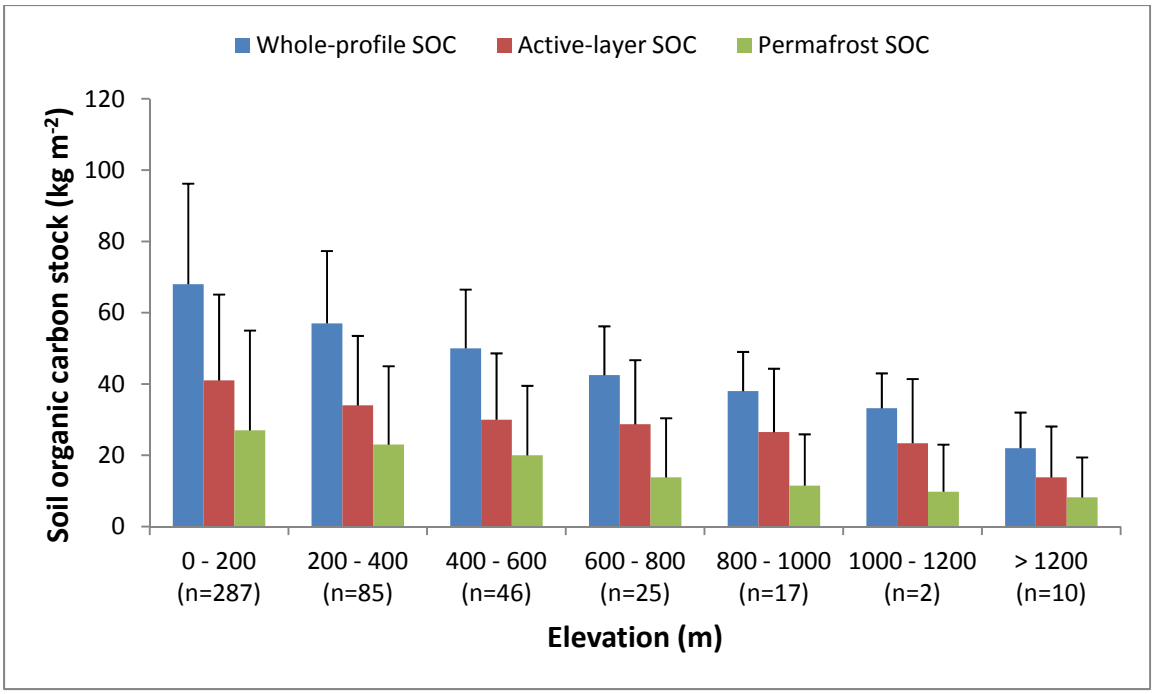

Figure 2.

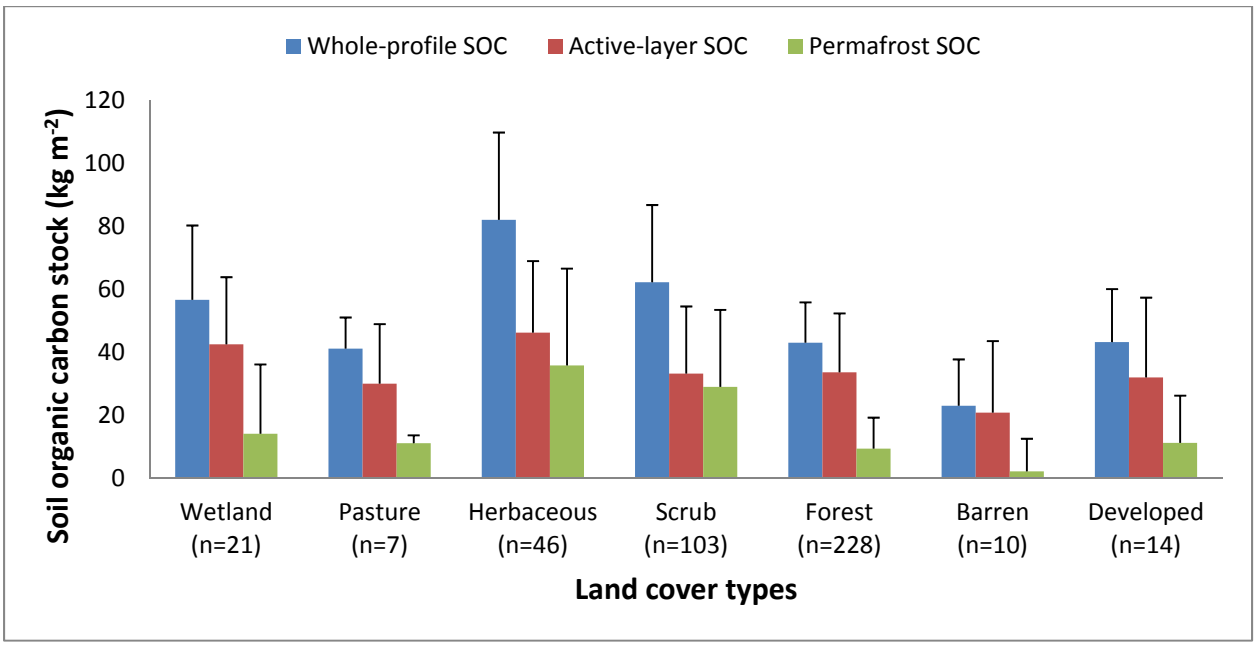

Figure 3.